

SIMPLE: Simulation-Based Policy Learning and Evaluation for Humanoid Loco-manipulation

Songlin Wei*, Zhenhao Ni*, Jie Liu*, Zhenyu Zhao*,
Junjie Ye, Hongyi Jing, Junkai Xia, Xiawei Liu, Michael Leong, Liang Heng,
Di Huang, Yue Wang[†]
USC Physical Superintelligence (PSI) Lab
* equal contribution, [†] corresponding author
<https://psi-lab.ai/SIMPLE>



Figure 1: **Humanoid Loco-manipulation in SIMPLE.** We introduce a comprehensive simulation benchmark designed to standardize the evaluation and training of humanoid foundation models. The framework features 60 diverse whole-body tasks across 50 indoor scenes, utilizing over 1,000 object assets. By coupling MuJoCo’s robust contact physics with Isaac Sim’s photorealistic rendering, SIMPLE provides built-in data collection pipelines and natively benchmarks state-of-the-art VLAs and WAMs (e.g., Ψ_0 [1], $\pi_{0.5}$ [2], DreamZero [3]).

Abstract: Humanoid foundation models are advancing faster than we can evaluate them. While real-world testing is expensive and difficult to reproduce, existing simulation benchmarks focus primarily on table-top or wheeled robots. A scalable and reproducible benchmark for whole-body humanoid loco-manipulation remains an open problem. To this end, we present SIMPLE, a unified simulation testbed for humanoid policy learning and evaluation. SIMPLE couples the accurate contact-rich dynamics of MuJoCo with the photorealistic rendering of IsaacSim. It provides a large-scale environment comprising 60 diverse whole-body tasks, 50 indoor scenes, and over 1,000 object assets. To facilitate scalable data collection, the framework integrates two data generation pipelines: automated trajectory generation via motion planning and a low-latency VR teleoperation interface. We further integrate and benchmark mainstream humanoid policies at scale in SIMPLE, including lightweight imitation networks, large vision-language-action (VLA) models, and recent world action models (WAMs). Our experiments reveal a strong correlation between policy performance in simulation and the real world. Furthermore, we demonstrate that policies trained on data collected in SIMPLE can be transferred zero-shot to physical humanoid robots un-

der similar settings, providing a robust and reproducible foundation for humanoid robotics research. We will open-source our entire codebase to the community.

Keywords: Humanoid Loco-Manipulation, Simulation-based Evaluation, Whole-body Foundation Models

1 Introduction

Robotic foundation models [4, 3, 2, 1] are advancing rapidly, demonstrating increasingly general behaviors. However, scaling these models is fundamentally constrained by evaluation. For tabletop and wheeled robots, standardized simulation benchmarks [5, 6, 7, 8] have greatly accelerated progress. Developing equivalent benchmarks for humanoid robots remains an open challenge. Humanoid loco-manipulation is inherently complex, requiring the tight coordination of dynamic locomotion, whole-body balancing, and fine-grained dexterous manipulation.

Currently, most humanoid foundation models are evaluated directly in the real world. While authentic, real-world evaluation is expensive, time-consuming, and notoriously difficult to reproduce. Consequently, conducting fair, side-by-side comparisons across different policies is a major challenge. Recent efforts to automate real-world evaluation via crowd-sourced rankings [9] or VLM-based reset policies [10] face scalability limits and potential biases. Simulation offers a scalable alternative [11], but existing platforms are highly fragmented. They either focus exclusively on tabletop manipulation [5, 6], ignoring locomotion and whole-body balancing, or on pure locomotion [12, 13], lacking diverse object interactions.

To address this fragmentation, we present **SIMPLE**, a comprehensive, full-stack simulation testbed designed for the extensive evaluation and fair comparison of humanoid policies. Instead of focusing on a narrow subset of skills, SIMPLE provides a large-scale environment dedicated to whole-body loco-manipulation. We design 60 diverse tasks, spanning rigid object pick-and-place, non-prehensile interaction, and articulated object manipulation. These tasks are set in 50 indoor scenes [14] utilizing over 1,000 object assets [15]. To support this scale with high fidelity, SIMPLE utilizes a hybrid architecture, coupling the accurate contact-rich dynamics of MuJoCo [16] with the photorealistic ray-traced rendering of Isaac Sim [17]. This dual-simulator approach ensures that policies trained in SIMPLE experience both the rigorous physical constraints of real-world locomotion and the complex visual diversity required for robust perception.

A standardized testbed must also support the full lifecycle of policy development. Beyond evaluation, SIMPLE facilitates scalable data collection by providing two built-in pipelines: automated trajectory generation driven by motion planners [18, 19], and a low-latency VR teleoperation interface for collecting human demonstrations. By standardizing these pipelines, SIMPLE eliminates the engineering overhead typically required to gather high-quality, whole-body demonstration data. Furthermore, the testbed integrates state-of-the-art lower-body controllers [20, 21] and offers a unified interface with native compatibility for mainstream vision-language-action (VLA) architectures, such as Ψ_0 [1], $\pi_{0.5}$ [2], and GR00T-N1.6 [4], as well as World-Action-Models (WAMs) like DreamZero [3] and other recent models [22, 23]. Crucially, SIMPLE is designed to be fully portable. This modularity enables researchers to easily extend the framework with new tasks, objects, environments, and policies.

We conduct extensive evaluations on SIMPLE to benchmark state-of-the-art policies at scale. Our experiments reveal a strong correlation between policy performance in simulation and in the real world. We further demonstrate that policies trained on data collected in SIMPLE can be transferred zero-shot to physical humanoid robots under similar settings. Our contributions are threefold:

- We introduce SIMPLE, a hybrid full-stack simulation framework standardizing the evaluation of humanoid loco-manipulation.
- We construct a large-scale loco-manipulation environment comprising 60 diverse tasks, over 1,000 objects, and 50 scenes, alongside built-in pipelines for automated and teleoperated data collection, yielding over 6,000 trajectories.

- We conduct extensive benchmarking of mainstream VLA and WAM policies, demonstrating strong sim-to-real correlation and effective zero-shot policy transfer.

2 Related Work

2.1 Robot Policy Evaluation in the Real World

Evaluating generalist policies [2, 4, 24, 25, 1] directly in the real world is the current standard but presents significant scalability challenges. Fair and reproducible evaluation requires multiple rollouts with meticulous environment resets, which are difficult to standardize and prone to human-operator bias. To address this, prior works have proposed using 3D-printable assets [26, 27] or centralized physical testbeds [28], though these still require substantial human supervision. While AutoEval [10] employs large language models (LLMs) to automate resets, the robustness of LLM-based physical interventions remains suboptimal. Alternatively, RoboArena [9] mitigates human bias via a decentralized, double-blind evaluation protocol. However, while effective for zero-shot testing on controlled tabletop setups with standardized datasets [29], this paradigm does not easily extend to humanoids. Because large-scale humanoid data is scarce, evaluating VLA models typically requires collecting in-domain demonstrations for policy fine-tuning prior to testing. Both collecting these demonstrations and conducting subsequent physical evaluations involve highly dynamic, full-body motions with heavy hardware, significantly increasing operational complexity and safety risks. Consequently, while real-world evaluation remains the gold standard, relying on it for the rapid, iterative development of humanoid policies is highly impractical.

2.2 Simulation-Based Benchmarks for Manipulation

Simulation provides a scalable, reproducible, and automated alternative to real-world testing [30]. Benchmarks such as RLBench [31] and LIBERO [7] have driven significant progress in tabletop single-arm manipulation, while platforms like RoboCasa [32], Behavior-1K [8], MolmoSpaces [33], and ManiSkill-HAB [34] have extended evaluation to mobile manipulation. Crucially, Simpler-Env [11] demonstrated that simulation can serve as a faithful proxy for real-world evaluation. By identifying and mitigating visual and control gaps, they showed that policy performance in simulation is highly correlated with real-world rankings. More recently, RoboTwin [5] introduced extensive domain randomization for bimanual tasks, and RoboVerse [6] unified multiple benchmarks within IsaacLab [35]. However, these platforms are typically built on physics engines or configurations optimized exclusively for fixed-base or wheeled robots [36]. Consequently, they lack the necessary physics support and integration for humanoid whole-body loco-manipulation.

2.3 Simulation for Humanoid Loco-Manipulation

Simulation has long been the primary paradigm for training robust humanoid locomotion policies before real-world deployment. Recent frameworks like AMO [20] and SONIC [21] leverage massively parallel reinforcement learning in IsaacGym [37] and IsaacLab [35] to train highly stable lower-body and whole-body tracking networks. These locomotion-focused policies are frequently deployed and evaluated in MuJoCo [16] due to its superior contact fidelity. However, while these environments excel at locomotion, they lack the diverse object assets, complex indoor scenes, and photorealistic rendering required to train and evaluate generalist foundation models. Conversely, platforms capable of high-fidelity rendering (such as those built on PhysX) often struggle to provide the accurate, high-frequency contact dynamics necessary for stable humanoid locomotion and delicate hand-object interaction. SIMPLE bridges this divide by natively building upon MuJoCo [16] for superior contact fidelity, ensuring compatibility with state-of-the-art locomotion policies, while coupling it with Isaac Sim’s photorealistic rendering [17]. To the best of our knowledge, SIMPLE is the first comprehensive, full-stack simulation testbed dedicated to whole-body humanoid loco-manipulation, seamlessly integrating data generation, policy learning, and standardized evaluation.

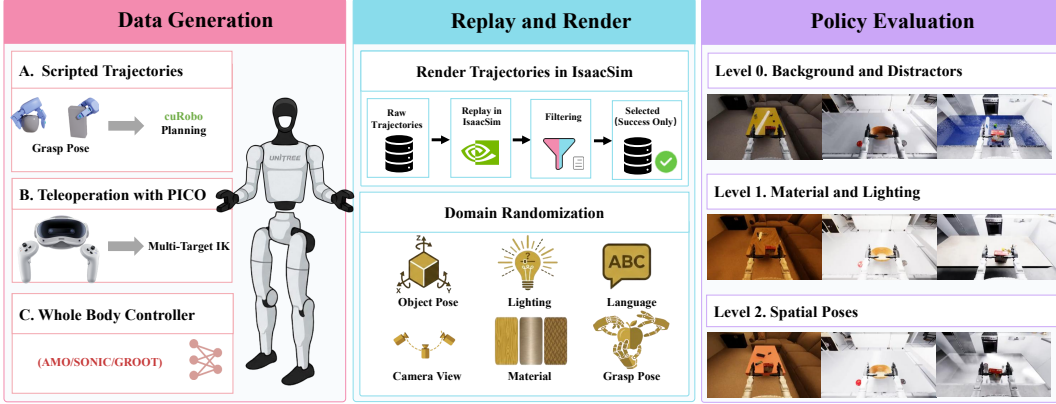


Figure 2: **System Pipeline.** Our pipeline consists of three stages: (1) data generation in MuJoCo via motion planning and teleoperation; (2) offline replay and rendering in Isaac Sim to obtain photorealistic visual observations; and (3) policy evaluation under diverse domain-randomized settings.

3 Method

We present SIMPLE, a comprehensive simulation infrastructure designed for humanoid loco-manipulation. The framework integrates dual-simulators for physics and rendering, large-scale asset curation, built-in data collection pipelines, and a standardized evaluation protocol. The overall system pipeline is illustrated in Fig. 2.

3.1 System Architecture

SIMPLE employs a dual-simulator architecture that strictly decouples physical simulation from visual rendering. As shown in Fig. 3, MuJoCo [16] handles all rigid-body dynamics, contact resolution, and robot control. At each simulation step, the physical states of the robot and environment are synchronized to Isaac Sim [17], which performs photorealistic ray-traced rendering. This separation allows SIMPLE to harness both the superior contact fidelity and locomotion stability of MuJoCo and the high-quality visual diversity of Isaac Sim.

To support generalist foundation models, SIMPLE implements a decoupled whole-body control scheme. The high-level policy (e.g., a VLA) predicts kinematic trajectories for the upper body and navigation commands for the base. These commands are subsequently passed to a state-of-the-art lower-body tracking controller [20, 21, 4], which operates at a higher frequency to maintain balance and execute locomotion. To ensure seamless integration with existing reinforcement learning workflows, the entire simulation loop is wrapped in a standard OpenAI Gym interface [38], as detailed in Algorithm 1.

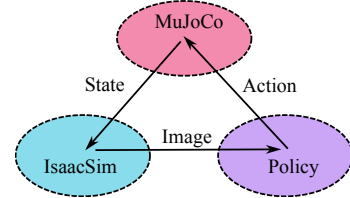


Figure 3: **System Diagram.** MuJoCo simulates physical interactions, while Isaac Sim synchronizes states and renders photorealistic images for policy inference.

Algorithm 1 Core Policy Evaluation Workflow in SIMPLE

```

1: import gymnasium as gym
2: env = gym.make("G1WholebodyXmovePickTeleop-v0",
3:   render_model="mujoco_isaacsim")
4: agent = Psi0Agent(env.robot)
5: env = LerobotEnv(env)
6: obs, info = env.reset()
7: while not (terminated or truncated) do
8:   action = agent.get_action(obs, info, instruction)
9:   obs, info, truncated, terminated = env.step(action)
10: end while
  
```

- ▷ Gym-style API
- ▷ Create Dual-Sim Env
- ▷ Instantiate VLA Agent
- ▷ Wrapper for trajectory recording
- ▷ Initialize environment
- ▷ 50 Hz control loop
- ▷ Policy inference
- ▷ Advance simulation

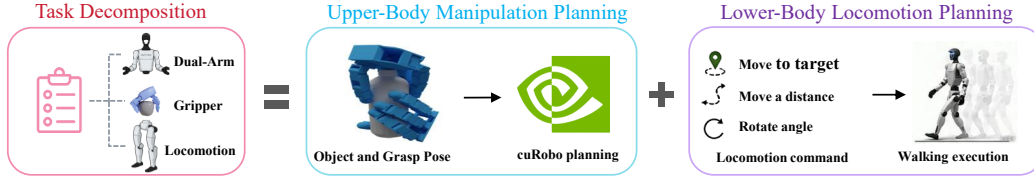


Figure 4: **Automated Motion Planning.** Based on task decomposition, scripted policies coordinate upper-body manipulation via motion planning and lower-body movement to generate automated demonstrations.

3.2 Large-Scale Asset Curation and Task Design

To ensure sufficient diversity for training robust vision-language-action models, we curated a massive library of objects and environments. We imported 53 objects from GraspNet-1B [26] and over 1,500 diverse objects from Objaverse [15]. To guarantee stable physics in MuJoCo, all object meshes underwent convex decomposition via CoACD [39] to generate accurate collision geometries. Simultaneously, all assets were converted into USD format with high-resolution textures for Isaac Sim rendering. To move beyond isolated tabletop setups, we integrated 50 complete indoor scenes from the HSSD dataset [14]. Using these assets, we designed 60 distinct whole-body loco-manipulation tasks, encompassing rigid object pick-and-place, non-prehensile interactions, and articulated object manipulation. Detailed illustrations of each task and other entities are included in the class diagrams provided in the Appendix.

3.3 Scalable Data Collection Pipelines

A core feature of SIMPLE is its built-in infrastructure for generating the large-scale demonstration data required to fine-tune humanoid policies. We provide two distinct pipelines: automated motion planning and human teleoperation.

Automated Motion Planning. For scalable trajectory generation, we implemented an automated pipeline driven by CuRobo [18], as illustrated in Fig. 4. To ensure physically plausible grasping, objects are first dropped in MuJoCo to determine their stable resting poses. These stable poses are then processed by BoDex [19] to synthesize feasible grasp configurations. During task execution, a scripted policy decomposes the high-level objective into atomic actions. CuRobo generates the kinematic trajectories for the dual arms to execute the grasp, while a scripted lower-body policy coordinates the necessary base movements to reach the target. We detail the grasp synthesis process and trajectory decomposition in the Appendix.

Low-Latency VR Teleoperation. Because motion planning struggles with complex dexterous manipulation, we also integrated a human teleoperation pipeline. To minimize latency, Isaac Sim rendering is disabled during data collection. Instead, MuJoCo’s native renderer streams egocentric stereo video directly to a PICO XR headset. The operator’s hand movements are retargeted to the humanoid’s upper body via inverse kinematics, while a whole-body tracking policy [20, 21] autonomously manages the robot’s balance and locomotion based on the operator’s joystick inputs. This decoupled approach drastically reduces the operator’s cognitive load. Demonstrations are recorded at 50 Hz and automatically exported into the standardized LeRobot format [40].

3.4 Offline Rendering and Domain Randomization

To close the visual sim-to-real gap, trajectories collected via motion planning or teleoperation are replayed offline in Isaac Sim. During this replay phase, we apply extensive domain randomization. We randomize object instances, initial poses, tabletop textures, lighting conditions, camera viewpoints, and language instructions. Specifically, we utilize NVIDIA vMaterials [41] to inject high-quality, diverse surface properties into the scenes. This offline rendering pipeline enables the generation of high-quality RGB observations under diverse visual conditions for downstream policy learning and evaluation.

3.5 Policy Integration and Evaluation Protocol

To standardize evaluation, SIMPLE defines a strict protocol with three progressively difficult levels. Level 1 introduces random distractor objects into the scene. Level 2 adds visual randomization, altering object materials and environmental lighting to test perceptual robustness. Level 3 introduces spatial randomization, varying the initial positions of both the target objects and the robot to evaluate layout generalization.

For policy integration, SIMPLE natively supports the Ψ_0 [1] training stack. The standard whole-body representation consists of a 32-dimensional proprioceptive state (14 DoF hands, 14 DoF arms, waist roll-pitch-yaw, and base height). The action space is 36-dimensional, comprising the 32-dimensional upper-body targets and 4-dimensional locomotion commands ($v_x, v_y, v_{yaw}, q_{yaw}$). Using this unified interface, we rendered 6,000 episodes to facilitate the large-scale benchmarking of mainstream VLA and WAM architectures.

4 Experiments

In this section, we evaluate the utility and scalability of the SIMPLE benchmark. We first present the results of our large-scale benchmarking, where state-of-the-art VLA models and WAMs are evaluated in a controlled environment across multiple tasks. We then assess the efficiency of our data generation pipelines. Next, we conduct ablation studies to analyze the impact of domain randomization, data scaling, and data sources on policy learning. Finally, we evaluate the feasibility of transferring policies trained entirely in SIMPLE to the real world in a zero-shot manner.

4.1 Large-Scale Benchmarking of Humanoid Policies

To benchmark state-of-the-art humanoid models, we select six representative tasks and evaluate them across the three domain-randomization levels defined in Section 3.5.

Baseline	XMovePick	BendPick	Handover	Mobile P&P	Grasp	XMoveBendPick
Ψ_0 [1]	10 / 10 / 6	10 / 10 / 10	7 / 7 / 10	7 / 5 / 6	10 / 10 / 8	<u>10 / 9 / 9</u>
GR00T N1.6 [4]	<u>10 / 10 / 7</u>	7 / 7 / 6	1 / 3 / 3	0 / 0 / 0	9 / 9 / 7	4 / 4 / 1
$\pi_{0.5}$ [2]	<u>7 / 5 / 1</u>	<u>10 / 10 / 8</u>	5 / 4 / 5	3 / 3 / 3	10 / 10 / 8	0 / 0 / 0
InternVLA [42]	0 / 0 / 0	<u>5 / 5 / 0</u>	0 / 0 / 0	0 / 0 / 0	0 / 0 / 0	3 / 5 / 7
H-RDT [23]	0 / 0 / 2	0 / 0 / 1	0 / 1 / 0	0 / 0 / 0	0 / 0 / 0	0 / 0 / 0
DreamZero [3]	10 / 10 / 10	9 / 9 / 8	<u>7 / 8 / 9</u>	5 / 3 / 3	9 / 10 / 7	0 / 0 / 1
EgoVLA [22]	0 / 1 / 2	7 / 5 / 8	<u>0 / 4 / 3</u>	0 / 0 / 0	<u>10 / 10 / 7</u>	3 / 5 / 4
DP [43]	3 / 3 / 2	10 / 8 / 6	3 / 2 / 4	4 / 0 / 0	8 / 9 / 8	0 / 0 / 0
ACT [44]	10 / 10 / 5	10 / 9 / 9	7 / 7 / 10	<u>5 / 5 / 5</u>	10 / 10 / 8	9 / 10 / 10

Table 1: **Benchmark Results.** Each entry reports performance under three domain-randomization levels (*Level 0 / Level 1 / Level 2*). The six representative tasks are XMovePickTeleop-v0, BendPickMP-v0, HandoverTeleop-v0, LocomotionPickBetweenTablesTeleop-v0, TabletopGraspMP-v0, and XMoveBendPickTeleop-v0, where the suffix *MP* denotes motion planning and *Teleop* denotes teleoperation. **Boldface** indicates the best performance, and underlined values indicate the second best.

Baselines. The evaluated baseline models are categorized into four groups: **(1) VLA Models.** Ψ_0 [1] is a 2.5B universal humanoid foundation model specialized for rapid adaptation through fine-tuning. We also evaluate $\pi_{0.5}$ [2] and GR00T-N1.6 [4], two seminal VLA models for general robotics, carefully adapting their pre-trained weights to the humanoid embodiment. **(2) Models Trained on Egocentric Video.** EgoVLA [22] and H-RDT [23] are two foundation models that are pre-trained or co-trained with human video data to leverage human manipulation priors for humanoid control. **(3) World-Action Models.** DreamZero [3] extends video generation models to simultaneously predict future video frames and actions. By imagining future interactions during execution, the video prediction mechanism serves as planning in image space. **(4) Imitation Learning Baselines.** Because

Collection Method	T1: Whole-Body Pick-Place		T2: Stand-Still Handover		T3: Mobile Pick-Place	
	Demos/hr \uparrow	Avg. time (s) \downarrow	Demos/hr \uparrow	Avg. time (s) \downarrow	Demos/hr \uparrow	Avg. time (s) \downarrow
Motion Planning (Sim)	58.9	61.1	32.7	109.8	24.0	150.0
Teleoperation (Real)	<u>206.8</u>	<u>17.4</u>	<u>130.9</u>	<u>27.5</u>	<u>87.2</u>	<u>41.3</u>
Teleoperation (Sim)	310.3	11.6	197.8	18.2	156.5	23.0

Table 2: **Data Collection Efficiency.** Each cell reports the number of demonstrations collected per hour and the mean episode duration in seconds. Motion planning runs without an operator; teleoperation figures reflect a single experienced operator per session.

our benchmark utilizes single-task fine-tuning, we also include two classic visual imitation learning baselines, Diffusion policy (DP) [43] and Action Chunk Transformers (ACT) [44].

Experimental Results. Additional details regarding the adaptation of each baseline are provided in the Appendix. As shown in Table 1, Ψ_0 consistently performs well across most tasks and leads the benchmark. DreamZero and $\pi_{0.5}$ demonstrate strong generalization performance on *level 2* across most tasks, with the exception of Task 6, likely because it requires highly precise base movements. Interestingly, the relatively small ACT model achieves strong overall performance, which we attribute to its data efficiency on the SIMPLE dataset, whose demonstrations are less noisy than real-world teleoperation data. Crucially, the simulation rankings for these baselines closely echo the real-world experiments reported in prior work [1], confirming that SIMPLE serves as a faithful proxy for real-world policy evaluation.

4.2 Data Collection Efficiency in the Simulator

A key motivation for building SIMPLE is to reduce the cost and effort of collecting high-quality robot demonstration data. We compare three data collection paradigms across three representative tasks: *whole-body pick-and-place* (T1), *stand-still handover* (T2), and *mobile pick-and-place* (T3). The three paradigms are: (1) **Motion planning (MP)** in simulation, which generates demonstrations autonomously without a human operator; (2) **Real-robot teleoperation**, where an operator collects demonstrations directly on physical hardware; and (3) **Sim teleoperation**, where a human operator controls the robot inside SIMPLE via the VR interface;

We measure collection throughput in demonstrations per hour (demos/hr) and average episode duration (seconds), as reported in Table 2. Motion planning achieves the lowest throughput due to the difficulty of optimization in high-dimensional spaces; however, it does not incur operator fatigue or hardware reset overhead. Real-robot teleoperation achieves higher efficiency and captures more natural whole-body motions than motion-planning-based scripted policies. Conversely, Sim teleoperation is substantially faster because it avoids physical reset overhead, safety constraints, and hardware maintenance. Beyond raw time efficiency, simulated data collection is fundamentally more scalable. It eliminates the need for physical humanoid hardware, requiring only a standard VR headset, and allows collected trajectories to be infinitely scaled across diverse environments, lighting conditions, and object instances via offline replay and rendering.

4.3 Ablation Studies

Domain Randomization and Data Scaling. Domain randomization (DR) is central to bridging the visual sim-to-real gap. We ablate the effect of training data composition on cross-level generalization using Ψ_0 fine-tuned for 2,000 steps. As reported in Table 3, training on Level 0 data alone yields a strong in-distribution success rate (0.80 at Eval Set 0) but generalizes poorly to harder visual conditions (0.50 at Eval Set 2). Mixing Level 0 and Level 1 training data maintains in-distribution performance while substantially improving out-of-distribution robustness (0.80 on Set 2). This confirms that exposure to diverse visual conditions during training is necessary for policies to transfer to challenging environments. The results motivate the mixed-DR evaluation strategy adopted in the main benchmark (Table 1). Furthermore, we found that increasing the amount of teleoperation data significantly improves performance across all three validation sets.

Task	Training data	Eval Set 0	Eval Set 1	Eval Set 2
BendHandover	10× Level 0	8/10 = 0.80	8/10 = 0.80	5/10 = 0.50
	5× Level 0 + 5× Level 1	8/10 = 0.80	7/10 = 0.70	8/10 = 0.80
XmoveBendPick	10 Trajectories (Teleop)	5/10 = 0.50	6/10 = 0.60	3/10 = 0.30
	100 Trajectories (Teleop)	10/10 = 1.00	9/10 = 0.90	9/10 = 0.90

Table 3: **Ablation Study on Domain Randomization.** Evaluation success rates of Ψ_0 fine-tuned for 2,000 training steps under different training data compositions. Training with mixed domain-randomization levels improves generalization to harder evaluation settings. Scaling up teleoperation data further improves performance.

Variant	BendPick	Mobile P&P	XMoveBendPick	Avg.	Task	Sim Eval	Real Eval
MP	10/10/10	3/2/2	4/2/2	5.00	Pick & Place	9/10 = 0.90	8/10 = 0.80
Teleop	8/8/6	7/5/6	10/9/9	7.56	Handover	10/10 = 1.00	8/10 = 0.80

Table 4: **Ablation Study on Data Source.** We compare motion-planning-only and teleoperation-only training data across three task families. Teleoperation data leads to better performance.

Table 5: **Zero-Shot Sim-to-Real Transfer.** Success rates of a single policy fine-tuned exclusively on simulation data, evaluated both in the simulator and directly in the real world.

Data Source Quality. To study the impact of different data sources, we fine-tune Ψ_0 [1] on three tasks using either motion-planning-only data or teleoperation-only data (Table 4). In general, human teleoperation data proves more suitable for learning complex tasks, which we attribute to its diverse and naturalistic motion profiles.

4.4 Zero-Shot Sim-to-Real Transfer

While SIMPLE is primarily designed as a simulation benchmark, we investigate whether policies trained exclusively on SIMPLE data can transfer to the real world. Because real-world evaluation is highly constrained, we perform this evaluation on a subset of tasks under similar environmental settings, as illustrated in Figure 5. As shown in Table 5, we observe that the learned Ψ_0 policy generalizes to the real world in a zero-shot fashion without requiring real-world data for downstream fine-tuning. This suggests that the high-fidelity physics and photorealistic rendering provided by SIMPLE are sufficient to cross the sim-to-real gap for certain loco-manipulation tasks.

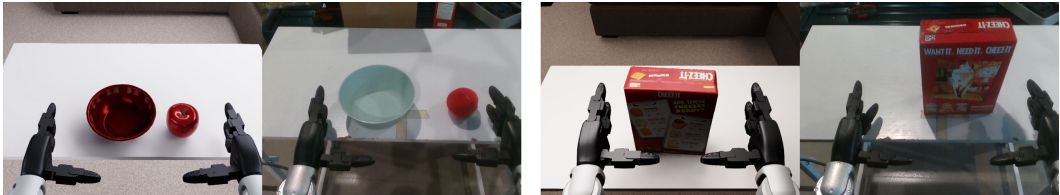


Figure 5: **Sim-to-Real Task Observations.** Each task is shown as an adjacent simulation–real pair, with the simulated egocentric view on the left and the corresponding real egocentric view on the right. The left pair shows the pick-and-place task, and the right pair shows the handover task.

5 Conclusion

We presented SIMPLE, a full-stack simulation infrastructure designed to standardize the evaluation and training of humanoid policies. By coupling the robust contact physics of MuJoCo with the photorealistic rendering of Isaac Sim, SIMPLE provides a high-fidelity environment tailored for whole-body loco-manipulation. The framework features a large-scale benchmark comprising 60 diverse tasks, over 1,000 objects, and 50 indoor scenes. To facilitate scalable policy learning, SIMPLE integrates built-in data collection pipelines for both automated motion planning and low-latency VR teleoperation. Our extensive benchmarking of state-of-the-art VLA and WAM architectures demonstrates that performance in SIMPLE strongly correlates with real-world outcomes, and that data

generated in SIMPLE empowers effective sim-to-real transfer. We hope SIMPLE will serve as a reproducible and scalable foundation to accelerate future research in humanoid robotics.

Limitations. Despite these contributions, SIMPLE has several limitations that point toward future work. (1) *Rendering throughput.* The photorealistic ray-tracing pipeline in Isaac Sim is computationally expensive. A single GPU renders ~ 4 frames per second, making large-scale dataset generation time-intensive. (2) *Rigid-body assumption.* The current simulation pipeline models all objects as rigid bodies. Deformable and soft-body objects such as cloth, rope, or food items cannot be faithfully simulated within the current framework.

References

- [1] S. Wei, H. Jing, B. Li, Z. Zhao, J. Mao, Z. Ni, S. He, J. Liu, X. Liu, K. Kang, et al. Ψ_0 : An open foundation model towards universal humanoid loco-manipulation. *arXiv preprint arXiv:2603.12263*, 2026.
- [2] P. Intelligence, K. Black, N. Brown, J. Darpinian, K. Dhabalia, D. Driess, A. Esmail, M. Equi, C. Finn, N. Fusai, et al. $\pi_{0.5}$: A vision-language-action model with open-world generalization. *arXiv preprint arXiv:2504.16054*, 2025.
- [3] S. Ye, Y. Ge, K. Zheng, S. Gao, S. Yu, G. Kurian, S. Indupuru, Y. L. Tan, C. Zhu, J. Xiang, et al. World action models are zero-shot policies. *arXiv preprint arXiv:2602.15922*, 2026.
- [4] J. Bjorck, F. Castañeda, N. Cherniadev, X. Da, R. Ding, L. Fan, Y. Fang, D. Fox, F. Hu, S. Huang, et al. Gr00t n1: An open foundation model for generalist humanoid robots. *arXiv preprint arXiv:2503.14734*, 2025.
- [5] T. Chen, Z. Chen, B. Chen, Z. Cai, Y. Liu, Z. Li, Q. Liang, X. Lin, Y. Ge, Z. Gu, et al. Robotwin 2.0: A scalable data generator and benchmark with strong domain randomization for robust bimanual robotic manipulation. *arXiv preprint arXiv:2506.18088*, 2025.
- [6] H. Geng, F. Wang, S. Wei, Y. Li, B. Wang, B. An, C. T. Cheng, H. Lou, P. Li, Y.-J. Wang, et al. Roboverse: Towards a unified platform, dataset and benchmark for scalable and generalizable robot learning. *arXiv preprint arXiv:2504.18904*, 2025.
- [7] B. Liu, Y. Zhu, C. Gao, Y. Feng, Q. Liu, Y. Zhu, and P. Stone. Libero: Benchmarking knowledge transfer for lifelong robot learning. *Advances in Neural Information Processing Systems*, 36:44776–44791, 2023.
- [8] C. Li, R. Zhang, J. Wong, C. Gokmen, S. Srivastava, R. Martín-Martín, C. Wang, G. Levine, M. Lingelbach, J. Sun, et al. Behavior-1k: A benchmark for embodied ai with 1,000 everyday activities and realistic simulation. In *Conference on Robot Learning*, pages 80–93. PMLR, 2023.
- [9] P. Atreya, K. Pertsch, T. Lee, M. J. Kim, A. Jain, A. Kuramshin, C. Eppner, C. Neary, E. Hu, F. Ramos, et al. Roboarena: Distributed real-world evaluation of generalist robot policies. In *Proceedings of the Conference on Robot Learning (CoRL 2025)*, 2025.
- [10] Z. Zhou, P. Atreya, Y. L. Tan, K. Pertsch, and S. Levine. Autoeval: Autonomous evaluation of generalist robot manipulation policies in the real world. *arXiv preprint arXiv:2503.24278*, 2025.
- [11] X. Li, K. Hsu, J. Gu, K. Pertsch, O. Mees, H. R. Walke, C. Fu, I. Lunawat, I. Sieh, S. Kirmani, et al. Evaluating real-world robot manipulation policies in simulation. *arXiv preprint arXiv:2405.05941*, 2024.
- [12] C. L. Lab. Humanoidverse: A multi-simulator framework for humanoid robot sim-to-real learning. <https://github.com/LeCAR-Lab/HumanoidVerse>, 2025.

- [13] C. Sferrazza, D.-M. Huang, X. Lin, Y. Lee, and P. Abbeel. Humanoidbench: Simulated humanoid benchmark for whole-body locomotion and manipulation, 2024.
- [14] M. Khanna, Y. Mao, H. Jiang, S. Haresh, B. Shacklett, D. Batra, A. Clegg, E. Undersander, A. X. Chang, and M. Savva. Habitat synthetic scenes dataset (hssd-200): An analysis of 3d scene scale and realism tradeoffs for objectgoal navigation. In *Proceedings of the IEEE/CVF Conference on Computer Vision and Pattern Recognition*, pages 16384–16393, 2024.
- [15] M. Deitke, D. Schwenk, J. Salvador, L. Weihs, O. Michel, E. VanderBilt, L. Schmidt, K. Ehsani, A. Kembhavi, and A. Farhadi. Objaverse: A universe of annotated 3d objects. In *Proceedings of the IEEE/CVF conference on computer vision and pattern recognition*, pages 13142–13153, 2023.
- [16] E. Todorov, T. Erez, and Y. Tassa. Mujoco: A physics engine for model-based control. In *2012 IEEE/RSJ international conference on intelligent robots and systems*, pages 5026–5033. IEEE, 2012.
- [17] NVIDIA. Isaac Sim. URL <https://github.com/isaac-sim/IsaacSim>.
- [18] B. Sundaralingam, A. Murali, and S. Birchfield. curobov2: Dynamics-aware motion generation with depth-fused distance fields for high-dof robots, 2026.
- [19] J. Chen, Y. Ke, and H. Wang. Bodex: Scalable and efficient robotic dexterous grasp synthesis using bilevel optimization. *arXiv preprint arXiv:2412.16490*, 2024.
- [20] J. Li, X. Cheng, T. Huang, S. Yang, R. Qiu, and X. Wang. Amo: Adaptive motion optimization for hyper-dexterous humanoid whole-body control. *Robotics: Science and Systems 2025*, 2025.
- [21] Z. Luo, Y. Yuan, T. Wang, C. Li, S. Chen, F. Castaneda, Z.-A. Cao, J. Li, D. Minor, Q. Ben, et al. Sonic: Supersizing motion tracking for natural humanoid whole-body control. *arXiv preprint arXiv:2511.07820*, 2025.
- [22] R. Yang, Q. Yu, Y. Wu, R. Yan, B. Li, A.-C. Cheng, X. Zou, Y. Fang, X. Cheng, R.-Z. Qiu, et al. Egovla: Learning vision-language-action models from egocentric human videos. *arXiv preprint arXiv:2507.12440*, 2025.
- [23] H. Bi, L. Wu, T. Lin, H. Tan, Z. Su, H. Su, and J. Zhu. H-rdt: Human manipulation enhanced bimanual robotic manipulation. In *Proceedings of the AAAI Conference on Artificial Intelligence*, volume 40, pages 18135–18143, 2026.
- [24] S. Deng, M. Yan, S. Wei, H. Ma, Y. Yang, J. Chen, Z. Zhang, T. Yang, X. Zhang, W. Zhang, et al. Graspvla: a grasping foundation model pre-trained on billion-scale synthetic action data. *arXiv preprint arXiv:2505.03233*, 2025.
- [25] J. Zhang, K. Wang, S. Wang, M. Li, H. Liu, S. Wei, Z. Wang, Z. Zhang, and H. Wang. Uni-navid: A video-based vision-language-action model for unifying embodied navigation tasks. *arXiv preprint arXiv:2412.06224*, 2024.
- [26] H.-S. Fang, C. Wang, M. Gou, and C. Lu. Graspnet-1billion: A large-scale benchmark for general object grasping. In *Proceedings of the IEEE/CVF conference on computer vision and pattern recognition*, pages 11444–11453, 2020.
- [27] S. Wei, H. Geng, J. Chen, C. Deng, C. Wenbo, C. Zhao, X. Fang, L. Guibas, and H. Wang. D³roma: Disparity diffusion-based depth sensing for material-agnostic robotic manipulation. In *ECCV 2024 Workshop on Wild 3D: 3D Modeling, Reconstruction, and Generation in the Wild*, 2024.
- [28] A. Yakefu, B. Xie, C. Xu, E. Zhang, E. Zhou, F. Jia, H. Yang, H. Fan, H. Zhang, H. Peng, et al. Robochallenge: Large-scale real-robot evaluation of embodied policies. *arXiv preprint arXiv:2510.17950*, 2025.

- [29] A. Khazatsky, K. Pertsch, S. Nair, A. Balakrishna, and S. D. et al. DROID: A Large-Scale In-The-Wild Robot Manipulation Dataset. In *Proceedings of Robotics: Science and Systems (RSS)*, 2024. doi:10.15607/RSS.2024.XX.120.
- [30] Y. R. Wang, C. Ung, G. Tannert, J. Duan, J. Li, A. Le, R. Oswal, M. Grotz, W. Pumacay, Y. Deng, et al. Roboeval: Where robotic manipulation meets structured and scalable evaluation. *arXiv preprint arXiv:2507.00435*, 2025.
- [31] S. James, Z. Ma, D. R. Arrojo, and A. J. Davison. Rlbench: The robot learning benchmark & learning environment. *IEEE Robotics and Automation Letters*, 5(2):3019–3026, 2020.
- [32] S. Nasiriany, S. Nasiriany, A. Maddukuri, and Y. Zhu. Robocasa365: A large-scale simulation framework for training and benchmarking generalist robots. In *International Conference on Learning Representations (ICLR)*, 2026.
- [33] Y. Kim, W. Pumacay, O. Rayyan, M. Argus, W. Han, E. VanderBilt, J. Salvador, A. Deshpande, R. Hendrix, S. Jauhri, S. Liu, N. M. M. Shafiullah, M. Guru, A. Guru, A. Eftekhari, K. Farley, D. Clay, J. Duan, P. Wolters, A. Herrasti, Y.-C. Lee, G. Chalvatzaki, Y. Cui, A. Farhadi, D. Fox, and R. Krishna. Molmospaces: A large-scale open ecosystem for robot navigation and manipulation, 2026.
- [34] A. Shukla, S. Tao, and H. Su. Maniskill-hab: A benchmark for low-level manipulation in home rearrangement tasks. *arXiv preprint arXiv:2412.13211*, 2024.
- [35] M. Mittal, P. Roth, J. Tigue, A. Richard, O. Zhang, P. Du, A. Serrano-Munoz, X. Yao, R. Zurbrugg, N. Rudin, et al. Isaac lab: A gpu-accelerated simulation framework for multi-modal robot learning. *arXiv preprint arXiv:2511.04831*, 2025.
- [36] Y. Chen, S. Wei, B. Xiao, J. Lyu, J. Chen, F. Zhu, and H. Wang. Robohanger: Learning generalizable robotic hanger insertion for diverse garments. *IEEE Robotics and Automation Letters*, 2025.
- [37] V. Makoviychuk, L. Wawrzyniak, Y. Guo, M. Lu, K. Storey, M. Macklin, D. Hoeller, N. Rudin, A. Allshire, A. Handa, et al. Isaac gym: High performance gpu-based physics simulation for robot learning. *arXiv preprint arXiv:2108.10470*, 2021.
- [38] G. Brockman, V. Cheung, L. Pettersson, J. Schneider, J. Schulman, J. Tang, and W. Zaremba. Openai gym. *arXiv preprint arXiv:1606.01540*, 2016.
- [39] X. Wei, M. Liu, Z. Ling, and H. Su. Approximate convex decomposition for 3d meshes with collision-aware concavity and tree search. *ACM Transactions on Graphics (TOG)*, 41(4):1–18, 2022.
- [40] R. Cadene, S. Aliberts, F. Capuano, M. Aractingi, A. Zouitine, P. Kooijmans, J. Choghari, M. Russi, C. Pascal, S. Palma, et al. Lerobot: An open-source library for end-to-end robot learning. *arXiv preprint arXiv:2602.22818*, 2026.
- [41] NVIDIA. vmaterials. <https://developer.nvidia.com/vmaterials>, 2026. Accessed: 2026-05-24.
- [42] X. Chen, Y. Chen, Y. Fu, N. Gao, J. Jia, W. Jin, H. Li, Y. Mu, J. Pang, Y. Qiao, et al. Internvlm1: A spatially guided vision-language-action framework for generalist robot policy. *arXiv preprint arXiv:2510.13778*, 2025.
- [43] C. Chi, Z. Xu, S. Feng, E. Cousineau, Y. Du, B. Burchfiel, R. Tedrake, and S. Song. Diffusion policy: Visuomotor policy learning via action diffusion. *The International Journal of Robotics Research*, 44(10-11):1684–1704, 2025.
- [44] T. Z. Zhao, V. Kumar, S. Levine, and C. Finn. Learning fine-grained bimanual manipulation with low-cost hardware. *arXiv preprint arXiv:2304.13705*, 2023.

Contents

1	Introduction	2
2	Related Work	3
2.1	Robot Policy Evaluation in the Real World	3
2.2	Simulation-Based Benchmarks for Manipulation	3
2.3	Simulation for Humanoid Loco-Manipulation	3
3	Method	4
3.1	System Architecture	4
3.2	Large-Scale Asset Curation and Task Design	5
3.3	Scalable Data Collection Pipelines	5
3.4	Offline Rendering and Domain Randomization	5
3.5	Policy Integration and Evaluation Protocol	6
4	Experiments	6
4.1	Large-Scale Benchmarking of Humanoid Policies	6
4.2	Data Collection Efficiency in the Simulator	7
4.3	Ablation Studies	7
4.4	Zero-Shot Sim-to-Real Transfer	8
5	Conclusion	8
5.1	System Architecture Details	13
5.1.1	Main Class Entities	13
5.1.2	Sequential Diagram	15
5.2	Offline Object Preprocessing Pipeline	15
5.3	Baseline Implementation Details	15
5.4	Whole-Body Controller Details	17
5.5	Extended Benchmark Results	18
5.6	Task Suite and Dataset Statistics	18

Supplementary Material

This document provides five supplementary sections. §5.1 details the SIMPLE class hierarchy and the per-step message-passing sequence between MuJoCo and Isaac Sim. §5.2 describes the offline asset preprocessing pipeline for physics collision geometries, USD rendering assets, and grasp synthesis. §5.3 gives the fine-tuning hyperparameters and embodiment adaptations for each evaluated baseline. §5.4 describes the two whole-body locomotion controllers (AMO and SONIC) integrated in SIMPLE. §5.5 reports Ψ_0 results on six additional tasks to validate learnability across the full task suite, followed by the complete task list and asset distribution.

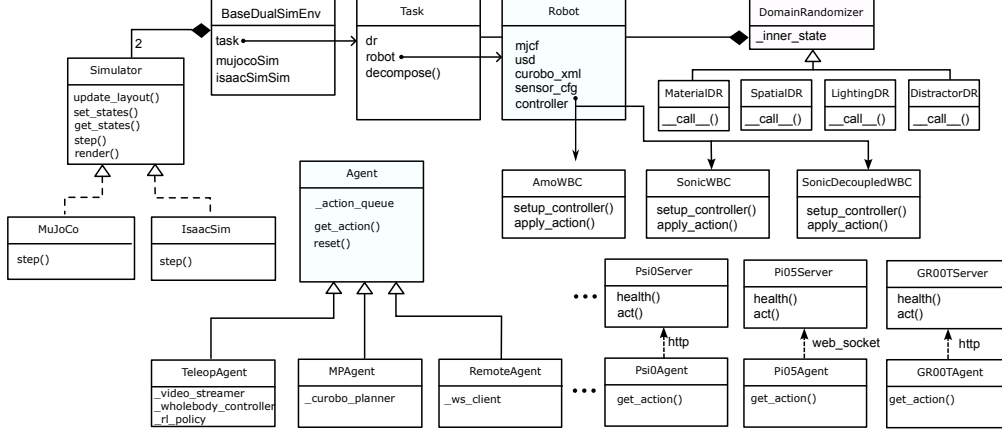


Figure 6: **Class Diagram of the SIMPLE Framework.** `BaseDualSimEnv` owns two `Simulator` instances and a `Task`, and exposes a standard Gym interface. `Task` composes a `DomainRandomizer` and a `Robot` and drives scene randomization at each reset. The `Agent` hierarchy (teleoperation, motion planning, remote inference) shares a unified `get_action` interface, while whole-body controllers (`AmoWBC`, `SonicWBC`, `SonicDecoupledWBC`) translate high-level commands into low-level joint targets. Policy servers (`PsiOAgent`, `PiO5Agent`, `GR00TAgent`) run as independent processes and are accessed over HTTP or WebSocket.

5.1 System Architecture Details

5.1.1 Main Class Entities

Figure 6 shows the class hierarchy of SIMPLE; we describe each component below.

BaseDualSimEnv. `BaseDualSim` (`envs/base_dual_env.py`) is the central `gymnasium.Env` that holds references to both a `MujocoSimulator` and an `IsaacSimSimulator`, along with the active `Task`. It initializes Isaac Sim lazily — the `SimulationApp` is created only when "isaac" appears in `sim_mode` — so MuJoCo-only workflows incur no rendering overhead. All concrete task environments (e.g., `LocoManipulationEnv`, `TabletopGraspEnv`) inherit from `BaseDualSim` and add task-specific `reset()` and `step()` logic on top.

Simulator. `Simulator` (`core/simulator.py`) is an abstract base class defining five operations: `update_layout()`, `set_states()`, `get_states()`, `step()`, and `render()`. `MujocoSimulator` (`engines/mujoco.py`) implements the physics backend: it runs the rigid-body contact simulation at 500 Hz and manages robot actuation, collision geometries, and proprioceptive state readout. `IsaacSimSimulator` (`engines/isaacsim.py`) implements the rendering backend: it consumes synchronized joint and pose states from MuJoCo and produces photorealistic ray-traced RGB frames via NVIDIA Isaac Sim’s USD/Replicator pipeline.

Task. `Task` (`core/task.py`) is an abstract class that bundles all task-specific configuration: the `DRManager` instance, the `Robot` descriptor, sensor configs, and Gym action/observation spaces. Its `reset()` method sequences through all registered randomizers — scene, target, container, distractor, spatial, lighting, camera, and material — building a `Layout` object that both simulators ingest to rebuild the scene. Concrete subclasses (e.g., `G1WholebodyXMovePickTaskTeleop`) additionally implement `check_success()`, a natural-language instruction property, and `decompose()` for automated subtask generation.

Robot. `Robot` (`core/robot.py`) is a configuration container that holds the MJCF physics model path, USD rendering model path, CuRobo kinematics config, sensor configurations, and controller config. Concrete implementations (e.g., `G1Wholebody`, `G1Sonic`) extend `Robot` with mixin traits such as `HeadCamMountable`, `HasDexterousHand`, and `CuRoboMixin`, and declare robot-specific

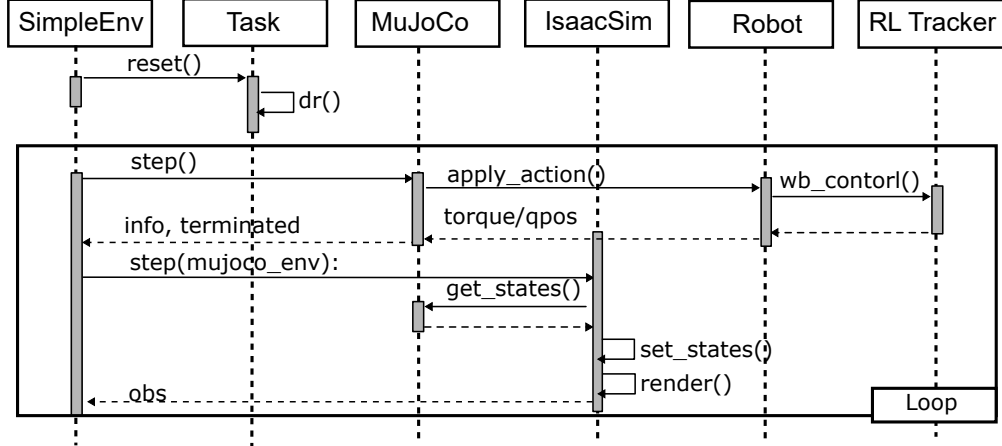


Figure 7: **Sequential Diagram of a Single `env.step()` Call.** Each invocation of `env.step(action)` (line 8 of Algorithm 1) triggers the following sequence: `MujocoSimulator` advances the physics loop at 500 Hz and writes the updated robot and object states to a shared buffer; `IsaacSimSimulator` reads those states, renders photorealistic RGB frames at 50 Hz, and returns the visual observation; `BaseDualSim` then queries the `Task` for the reward and termination condition before surfacing the full step output to the agent.

constants like joint names and default poses. The `Robot` class does not execute control directly; it passes its asset paths to the `Simulator` backends and its kinematics config to the whole-body controller modules.

DomainRandomizer. `DRManager` (`dr/manager.py`) maintains a named registry of `Randomizer` instances and dispatches randomization calls at each `Task.reset()`. Its `set_level()` method adjusts active configurations to one of three difficulty levels: Level 0 adds distractor objects and background variation, Level 1 additionally randomizes material shaders and lighting, and Level 2 further varies object and robot spatial poses. Four leaf randomizers each implement a `__call__()` interface: `MaterialDR` samples NVIDIA `vMaterials` surface shaders, `SpatialDR` varies object and robot initial poses, `LightingDR` randomizes light positions and intensities, and `DistractorDR` populates the scene with randomly chosen distractor objects.

Agent. `BaseAgent` (`agents/base_agent.py`) is the abstract policy interface; all subclasses implement `get_action(observation, instruction)` and manage an internal `_action_queue` that buffers predicted action chunks for step-by-step execution. `MotionPlanAgent` (`agents/mp_agent.py`) wraps a `CuRobo` planner: it converts the planned kinematic trajectory into a sequence of `ActionCmd` objects and replays them deterministically, enabling fully automated data collection without a human operator. `PicoDecoupledAgent` (`agents/pico_decoupled_agent.py`) is the teleoperation agent: it streams egocentric stereo video to a PICO XR headset via `TCPVideoSender`, receives hand-pose commands retargeted through inverse kinematics, and routes the resulting upper-body targets through the decoupled WBC pipeline.

RemoteAgent. VLA and WAM policies run as independent server processes (`Psi0Server`, `Pi05Server`, `GR00TServer`), each exposing a `health()` readiness check and an `act()` inference endpoint over HTTP or WebSocket. The corresponding client-side agents (`Psi0Agent`, `Pi05Agent`, `Gr00tN16Agent`) package RGB observations and proprioceptive state into the server’s expected format, issue a blocking network call, and enqueue the returned action chunk into the shared `_action_queue`. This server–client split allows policies to run on separate GPUs or machines, decoupling inference throughput from the simulation host’s memory budget.

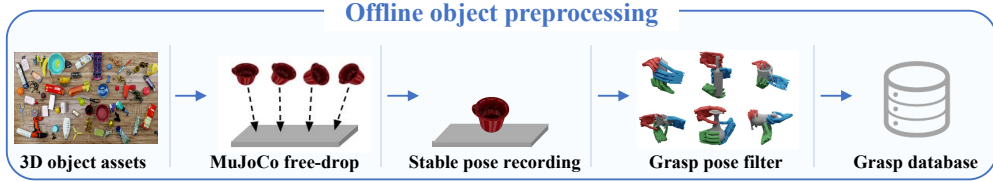


Figure 8: **Offline Object Preprocessing Pipeline.** Raw mesh assets from Objaverse and GraspNet-1B are processed for two purposes: (1) *For Physics* — CoACD convex decomposition generates MuJoCo collision geometries, and stable resting poses are determined by dropping each object in simulation; (2) *For Rendering* — meshes are converted to USD format with high-resolution PBR textures for Isaac Sim. BoDex [19] synthesizes dexterous grasp poses on the stable-pose meshes; the results are cached alongside each asset for use at task initialization.

Whole-Body Controllers. SIMPLE supports three whole-body controller (WBC) implementations, each following a common `setup_controller()` / `apply_action()` interface. AmoWBC wraps the AMO controller [20], which decouples upper- and lower-body control and uses a learned velocity-tracking policy for the base while accepting end-effector targets for the arms. SonicWBC (`agents/sonic_wbc_agent.py`) and SonicDecoupledWBC (`agents/sonic_decoupled_wbc_agent.py`) both build on the SONIC framework [21]: the former forwards raw whole-body motion-tracking commands via the Unitree SDK, while the latter instantiates the full `decoupled_wbc` pipeline — including a G1 kinematic model and a WBC policy — to convert high-level joint targets into low-level position commands at 50 Hz.

5.1.2 Sequential Diagram

Figure 7 expands `env.step(action)` (line 8 of Algorithm 1) into its internal message-passing sequence. Within each step, `MujocoSimulator` integrates physics at 500 Hz and writes updated states to a shared buffer; `IsaacSimSimulator` reads those states and renders RGB frames at 50 Hz; and `BaseDualSim` queries the `Task` for the reward and termination signal before returning the step output. This producer–consumer ordering ensures every inference step receives a physically consistent, photorealistic observation while allowing MuJoCo to sub-step ahead of the slower rendering pass.

5.2 Offline Object Preprocessing Pipeline

Figure 8 shows the offline preprocessing pipeline that runs once per asset and produces all artifacts needed for physics, rendering, and grasp planning.

Assets are drawn from Objaverse [15] (1,500+ objects) and GraspNet-1B [26] (75 objects). After normalization, each mesh is processed in two parallel tracks: the *physics track* applies CoACD [39] convex decomposition to generate MuJoCo collision geometries and drops each object in simulation to enumerate stable resting poses; the *rendering track* converts meshes to USD format with high-resolution PBR textures for Isaac Sim.

BoDex [19] synthesizes dexterous grasp configurations for each stable pose offline, caching quality scores and approach depths per asset. At task initialization, SIMPLE samples a stable pose via `SpatialDR`, retrieves the cached grasps, and passes the selected target to CuRobo [18] for trajectory generation — no online grasp synthesis is required at training or evaluation time.

5.3 Baseline Implementation Details

Ψ_0 [1] is a 2.5B humanoid foundation model with a Qwen3-VL-2B vision backbone and a flow-matching diffusion transformer action expert. We fine-tune the released pre-trained checkpoint for 40,000 steps on 8 NVIDIA A100 GPUs using DDP, with a per-device batch size of 16, a cosine-annealed learning rate of 1×10^{-4} , 1,000 warmup steps, and bf16 mixed precision. The action

head is configured with a 36-dimensional output and a chunk size of 30, matching the SIMPLE whole-body action space.

DreamZero [3] extends the Wan2.1-I2V video generation model (14B parameters) to jointly predict future video frames and robot actions via a flow-matching DiT action head, enabling planning in image space during execution. We initialize from the *DreamZero-AgiBot* pretrained checkpoint and apply LoRA fine-tuning (rank 4, α 4, targeting `q,k,v,o,ffn.0,ffn.2` layers) for 40,000 steps on eight NVIDIA A100 GPUs using DeepSpeed ZeRO-2, with a per-device batch size of 1, a cosine-annealed learning rate of 1×10^{-4} , and a 5% linear warmup. The action head outputs a 36-dimensional action at a step horizon of 48; video observations are rendered at 320×176 resolution and encoded by the Wan2.1 VAE, with the number of context frames set per task (17, 25, or 33 frames corresponding to chunk sizes of 2, 3, or 4, respectively).

$\pi_{0.5}$ [2] shows strong generalization on mobile dual-arm platforms, but its released checkpoint supports only a 30-dimensional action space. We expand the action dimension to 36 with a chunk size of 16, padding the weights of the affected linear layers to accommodate the larger space. To bridge the embodiment gap between the original training distribution and humanoid morphologies, we raise the learning rate from 1×10^{-5} to 1×10^{-4} and the global batch size from 32 to 128, fine-tuning from the *Pi05_DROID* checkpoint ported to PyTorch.

GR00T N1.6 [4] is a 3B VLA pretrained for general robot manipulation. We fine-tune from the released checkpoint for 20,000 steps on three NVIDIA A100 GPUs (global batch size 24, lr 1×10^{-4} cosine), using all default hyperparameters. As the RTC inference code is unavailable, we use a standard sequential scheme conditioning each prediction on the most recently executed observation.

InternVLA-M1 [42] integrates spatial grounding and robot control in a unified framework, but its pre-training on spatial reasoning and robotic-arm data limits direct transfer to humanoid tasks. Starting from the RT-1 Bridge checkpoint, we freeze the VLM backbone and fine-tune only the action head for 30,000 steps at a batch size of 64 on a single NVIDIA A100 GPU. InternVLA-M1 exhibits action jitter across consecutive chunks in our experiments, resulting in unstable executions.

H-RDT [23] is a 2B-parameter DiT-based action model trained for 10,000 steps with a batch size of 32 on a single NVIDIA A100 GPU. The resulting policy handles tasks that do not require precise movements well, but struggles with manipulation tasks that demand high joint-level accuracy across many degrees of freedom.

EgoVLA [22] is a vision–language–action model pre-trained on egocentric human manipulation videos using EgoDex and additional data sources. Because the original codebase predicts only end-effector wrist and hand poses, we adapt the action decoder to output the robot joint-space commands required by downstream tasks. We fine-tune on our teleoperated data for 115 epochs with an effective batch size of $16 \times 8 \times 4$, following the training configuration reported in the original paper. EgoVLA shows limited performance on lower-body commands, likely because its pre-training distribution emphasizes upper-body and hand manipulation and does not provide strong priors for coordinated lower-body locomotion.

Diffusion Policy (DP) [43] uses a pre-trained ResNet-18 as the visual encoder, with a learning rate of 1×10^{-4} and a global batch size of 32. Training runs for 40,000 steps on two NVIDIA A100 GPUs, taking approximately 15 hours per task. Despite fitting the training data reasonably, DP fails on most evaluation tasks; we attribute this to the insufficient visual capacity of the UNet-based architecture for the diverse visual conditions in SIMPLE. At inference time, we perform 100 denoising steps to recover actionable trajectories from noise.

Action Chunking with Transformers (ACT) [44] is reconfigured with a 36-dimensional action head and a chunk size of 100, using a transformer comprising 4 encoder layers and 1 decoder layer following the publicly released LeRobot configuration [40]. All other hyperparameters are kept identical to those used for DP.

Table 6: Representative tasks in our benchmark.

Task Name	Category	Teleop	Success Criteria
BendPick	Rigid	Yes	Lift the target object more than 5 cm from the table.
BendPickAndPlace	Rigid	Yes	Place the target object into the container.
BendHandover	Bimanual	Yes	Handover the object and place it into the container.
Handover	Bimanual	Yes	Handover the object and place it into the container.
OpenTrashCan	Articulated	Yes	Open the trash can lid beyond the target angle threshold.
PushOfficeChair	Non-prehensile	Yes	Push the office chair beyond the target distance.
OpenFaucet	Articulated	Yes	Rotate the faucet handle beyond the target angle.
OpenOven	Articulated	Yes	Open the oven door beyond the target angle threshold.
CloseDoor	Articulated	Yes	Close the door to the target closed state.
XMovePick	Mobile	Yes	Move laterally and lift the target object.
XMoveBendPick	Mobile	Yes	Move laterally, bend down, and lift the target object.
LocomotionPickBetweenTables	Whole-body	Yes	Transfer the object from one table to another table container.
PickAndPlaceAndHugContainer	Whole-body	Yes	Place two objects into the container, lift it, and move it onto another table.
BendPickMP	Rigid	No	Lift the target object more than 5 cm from the table.
TableTopGraspMp	Rigid	No	Lift the target object more than 5 cm from the table.
LocoPickBetweenTablesMP	Whole-body	No	Transfer the object from one table to another table.

5.4 Whole-Body Controller Details

SIMPLE integrates two whole-body locomotion controllers that share a common teleoperation interface but differ in their internal control architecture. Both controllers receive the same high-level inputs — upper-body joint targets from the teleoperation or policy layer and a 4-dimensional navigation command $(v_x, v_y, v_{yaw}, q_{yaw})$ — and output low-level joint position commands to the Unitree G1 at 500 Hz via MuJoCo.

AMO [20] adopts a decoupled architecture that treats upper-body and lower-body control as two independent problems. The lower body is governed by a learned RL locomotion policy (`AMO_Policy` in `robots/policy/AMO_Policy.py`) that takes IMU measurements and proprioceptive joint states as input and outputs 15 lower-body joint targets (hip, knee, ankle, and waist joints) at high frequency. The upper body is controlled separately by directly tracking the joint targets received from the high-level policy or teleoperator, so arm and hand movements do not feed back into the locomotion policy, giving the operator more predictable upper-body control at the cost of tighter coupling between arm posture and balance.

SONIC [21] takes an end-to-end whole-body motion tracking approach. SIMPLE provides two SONIC-based implementations: `SonicWbcAgent` (`agents/sonic_wbc_agent.py`), which forwards whole-body commands directly through the Unitree SDK bridge (`gear_sonic`), and `SonicDecoupledWbcAgent` (`agents/sonic_decoupled_wbc_agent.py`), which runs the full `decoupled_wbc` pipeline internally — instantiating a G1 kinematic model and a WBC policy — to convert upper-body joint targets and navigation commands into full-body position commands at

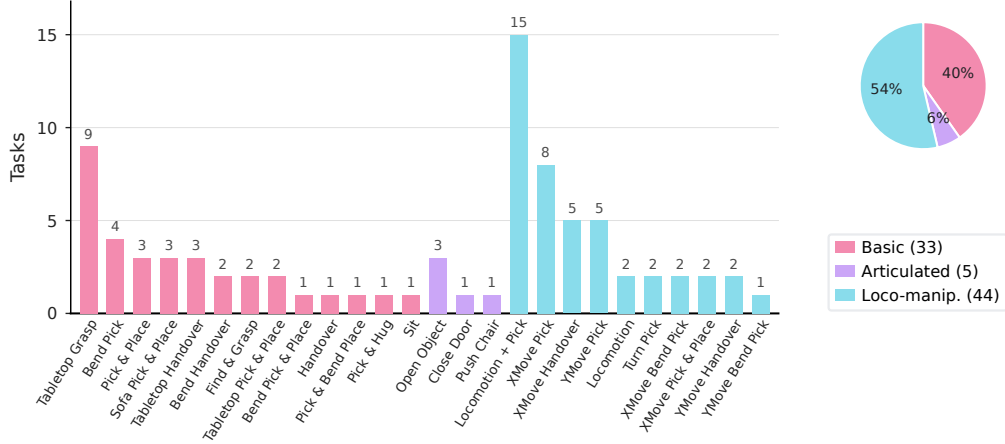


Figure 9: **Task Distribution.** Distribution of all tasks across three types: basic rigid pick-and-place, articulated object manipulation, and whole-body loco-manipulation.

50 Hz. Because SONIC tracks the operator’s whole-body motion as a unified trajectory rather than handling each segment independently, it tends to produce smoother and more natural whole-body demonstrations, particularly for tasks requiring coordinated arm–leg movements such as mobile pick-and-place.

5.5 Extended Benchmark Results

Table 7 reports Ψ_0 [1] success rates on six tasks beyond the main benchmark (Table 1), across all three DR levels (Level 0 / Level 1 / Level 2). These tasks cover articulated manipulation (CloseDoor, OpenOven, OpenFaucet, OpenTrashCan), non-prehensile interaction (PushOfficeChair), and bimanual rearrangement (PickAndPlaceAndHugContainer).

Table 7: Task suite results.

Baseline	CloseDoor	OpenOven	OpenFaucet	P&P&HugContainer	PushOfficeChair	OpenTrashCan
Ψ_0 [1]	10 / 10 / 10	7 / 5 / 4	3 / 3 / 4	7 / 6 / 3	10 / 10 / 10	7 / 9 / 9

Tasks with unambiguous geometric success signals (CloseDoor, PushOfficeChair) achieve 10/10/10 across all DR levels. Fine-grained contact tasks (OpenFaucet) reach 3–4/10, confirming a meaningful difficulty gradient. Articulated tasks (OpenOven, OpenTrashCan) degrade gracefully with DR level, consistent with the main benchmark trend. These results confirm every SIMPLE task is learnable and establish Ψ_0 as a reference baseline for future comparisons. The full task list with success criteria appears in Table 6.

5.6 Task Suite and Dataset Statistics

Table 6 lists representative tasks from the 60-task suite, with their skill category, collection modality, and programmatic success criterion. Teleoperated tasks cover dexterous or contact-rich behaviors (handovers, articulated objects) where motion planning yields unnatural trajectories; MP tasks cover pick-and-place motions solvable by CuRobo from stable grasp poses.

Figure 9 shows the task distribution across four humanoid capability axes: rigid grasping and placement, non-prehensile pushing, precise articulated-object control, and whole-body loco-manipulation requiring arm–leg coordination across spatial extents beyond single-arm reach.